

1 **Refined mapping of tree cover at fine-scale using time-series**  
2 **Planet-NICFI and Sentinel-1 imagery for Southeast Asia (2016-**  
3 **2021)**

4 Feng Yang<sup>a</sup>, Zhenzhong Zeng<sup>a,\*</sup>

5 <sup>a</sup> School of Environmental Science and Engineering, Southern University of Science and Technology,  
6 Shenzhen 518055, China

7

8

9 \* Correspondence to: [zengzz@sustech.edu.cn](mailto:zengzz@sustech.edu.cn) (Zhenzhong Zeng)

10 Mailing Address:

11 College of Engineering N808

12 Southern University of Science and Technology

13 Shenzhen, China

14

15

16

17

The manuscript for *Earth System Science Data*

18

~~August 10~~, 2023

19

Deleted: July

Deleted: 31

22 **Abstract:**

23 High-resolution mapping of tree cover is indispensable for effectively addressing tropical forest carbon loss,  
24 climate warming, biodiversity conservation, and sustainable development. However, the availability of  
25 precise high-resolution tree cover map products remains inadequate due to the inherent limitations of  
26 mapping techniques utilizing medium-to-coarse resolution satellite imagery, such as Landsat and Sentinel-2  
27 imagery. In this study, we have generated an annual tree cover map product at a resolution of 4.77 m for  
28 Southeast Asia (SEA) for the years 2016-2021 by integrating Planet-Norway's International Climate &  
29 Forests Initiative (NICFI) imagery and Sentinel-1 Synthetic Aperture Radar data. We have also collected  
30 annual tree cover/non-tree cover samples to assess the accuracy of our Planet-NICFI tree cover map product.  
31 The results show that our Planet-NICFI tree cover map product during 2016-2021 achieve high accuracy,  
32 with an overall accuracy of  $\geq 0.867 \pm 0.017$  and a mean F1 score of 0.921, respectively. Furthermore, our tree  
33 cover map product exhibits high temporal consistency from 2016 to 2021. Compared to existing map products  
34 (FROM-GLC10, ESA WorldCover 2020 and 2021), our tree cover map product exhibits better performance,  
35 both statistically and visually. Yet, the imagery obtained from Planet-NICFI performs less in mapping tree  
36 cover in areas with diverse vegetation or complex landscapes due to insufficient spectral information.  
37 Nevertheless, we highlight the capability of Planet-NICFI imagery in providing quick and fine-scale tree  
38 cover mapping to a large extent. The consistent characterization of tree cover dynamics in SEA's tropical  
39 forests can be further applied in various disciplines. Our data from 2016 to 2021 at a 4.77 m resolution are  
40 publicly available at <https://cstr.cn/31253.11.sciencedb.07173> (Yang and Zeng, 2023).

41

42 **1 Introduction**

43 Forests and tree-based systems outside forests play a crucial role in land-based carbon emissions or removals,

44 making them essential for supporting and monitoring the implementation of the Reducing Emissions from  
45 Deforestation and Forest Degradation (REDD+) and other land-based activities under the Paris Agreement  
46 (Skea et al., 2022; CoP26, 2021; FAO, 2020). However, current forest cover map products exhibit large errors  
47 in accurately estimating forest area and change, particularly in areas such as trees outside forests and forest  
48 edge landscapes (Mugabowindekwe et al., 2023; Reiner et al., 2023; Brandt et al., 2020). As a result, there is  
49 a growing demand for timely, high-quality, and high-resolution tree cover map products to accurately capture  
50 the dynamics and changes in forest cover.

Deleted: significant

51  
52 Many tree cover map products have been developed at medium-to-coarse resolutions (10-500 m), such as  
53 Finer Resolution Observation and Monitoring of Global Land Cover 10 m (FROM-GLC10; Gong et al.,  
54 2019), Environmental Systems Research Institute (ESRI) Land Cover (2017-2021) (Karra et al., 2021),  
55 European Space Agency (ESA) WorldCover 2020 and 2021 (Zanaga et al., 2022; Zanaga et al., 2021), GFC  
56 (Hansen et al., 2013), Globeland30 (Chen et al., 2015), Copernicus Global Land Service (CGLS) Land Cover  
57 (Buchhorn et al., 2020), ESA Climate Change Initiative (CCI)(ESA, 2017) and the National Aeronautics and  
58 Space Administration (NASA) MCD12Q1 (Friedl and Sulla-Menashe, 2019). However, accurate high-  
59 resolution tree cover map products at continental-to-global scales are still lacking due to mapping through  
60 medium-to-coarse resolution imagery (Zanaga et al., 2021; Hansen et al., 2010). Consequently, some  
61 uncertainties occur in acquiring global tree inventories and monitoring forest disturbances (deforestation and  
62 forest degradation). This is mainly due to isolated trees or long narrow forest cover removal (Reiner et al.,  
63 2023; Wagner et al., 2023; Sexton et al., 2016; Hammer et al., 2014; Hsieh et al., 2001).

64  
65 Only recently have two tree cover map products at <4.77 m been produced over Africa and the state of Mato

Deleted: from preprints

68 Grosso in Brazil using Planet-Norway's International Climate & Forests Initiative (NICFI) imagery based on  
69 deep learning algorithms (Reiner et al., 2023; Wagner et al., 2023). However, these two maps have only  
70 limited temporal or spatial coverage that occurred. Since the early 21st century, agricultural expansion has  
71 created a new wave of drastic land use/land cover changes in Southeast Asia (SEA), leading the region to be  
72 one of the most deforested regions worldwide (Zeng et al., 2018a; Zeng et al., 2018b; Achard et al., 2014).  
73 Average elevations and slopes of forest loss sites have significantly increased in SEA, particularly in the  
74 2010s, geometrically irregular upland land use sites commonly occur (Velasco et al., 2022; Feng et al., 2021).  
75 However, existing tree cover map products have underestimated deforestation (25-116%) and upland  
76 agricultural expansion rates (9-113%), especially on the topographic boundaries in SEA (Zeng et al., 2018a).  
77 Thus, fine-resolution tree cover map products in SEA, with high spatial resolution and longer consistent time  
78 series, are urgently needed to accurately monitor tree cover loss and related illegal deforestation. In addition,  
79 combining high-resolution optical imagery and Synthetic Aperture Radar (SAR) data (e.g., Sentinel-1) to  
80 produce large-area tree cover map products is still in its early stage (Zanaga et al., 2022; Karra et al., 2021;  
81 Zanaga et al., 2021; Buchhorn et al., 2020; Hansen et al., 2010).

82  
83 Concurrently, advances in large-scale cloud computing (e.g., Google Earth Engine, GEE; Gorelick et al.,  
84 2017) and available high-resolution satellite imagery (Roy et al., 2021) can facilitate the development of  
85 high-resolution and longer time-series tree cover map products at continental-to-global scales. In this paper,  
86 we generated a state-of-the-art fine-scale open-source tree cover map product for SEA during 2016-2021  
87 using Planet- NICFI imagery, Sentinel-1 SAR data, and the random forest (RF) method from a previous study  
88 (Yang et al., 2023). This dataset allows for extensive assessments of forest dynamics change, such as  
89 deforestation, forest degradation, and reforestation. In addition, our dataset can monitor trees outside forests

90 and long narrow forest cover removal, thus improving the accuracy of automated continental tree inventories,  
91 which helps optimize REDD+ under the Paris Agreement.

92

## 93 **2 Materials and methods**

### 94 **2.1 Satellite imagery**

95 We utilized Planet-NICFI and Sentinel-1 imagery for the years 2016-2021 to generate a time series tree cover  
96 map product for SEA. The Planet-NICFI program provides high-resolution (4.77 m per pixel) optical  
97 PlanetScope surface reflectance mosaics specifically designed for the tropics. These mosaics offer accurate  
98 and reliable spatial data with minimized effects from atmosphere and sensor characteristics, making them an  
99 ideal 'ground truth' representation (Planet Team, 2017). The mosaics cover the best imagery to represent every  
100 part of the coverage area during leaf-on periods from June to November based on cloud cover and acutance  
101 (image sharpness). The Planet-NICFI imageries consist of four bands: red, green, blue, and near-infrared, and  
102 cover a time period from 2015 to 2020 at bi-annual resolution for the archive, and from 2020 to 2023 at  
103 monthly resolution for monitoring purposes. We accessed and utilized these products in the GEE platform by  
104 authorizing our NICFI account to the GEE account.

105

106 We utilized Sentinel-1 on the GEE platform, specifically the 10 m resolution dual-polarization Ground Range  
107 Detected (GRD) scenes (VV + VH). We chose Sentinel-1 SAR imagery to correct cases of overestimation  
108 caused by confusion with herbaceous vegetation, or underestimation due to optical satellite observations  
109 omitting deciduous or semi-deciduous characteristics (Shimada et al., 2014). The SAR imagery, available  
110 every 12 days for a single satellite or 6 days for a dual-satellite constellation from October 2014 to the present,  
111 was pre-processed with the Sentinel-1 Toolbox for thermal noise removal, radiometric calibration, and terrain

112 correction.

113

## 114 **2.2 Validation dataset collection**

115 We collected time series validation datasets to assess the tree cover map product during 2016-2021, except  
116 for 2019 as it has been provided by Yang et al. (2023). Our mapping approach has been comprehensively  
117 assessed after being developed in 2019 (Yang et al., 2023). However, despite the advancements in the Land  
118 Cover Land Use Change (LCLUC) community, a notable gap remains the absence of publicly available high-  
119 resolution (e.g.,  $\leq 10$  m) tree cover/non-tree cover labels. The existing coarse-resolution labels for tree  
120 cover/non-tree cover can introduce considerable uncertainties when evaluating high-resolution tree cover  
121 maps. As a result, our ability to delve deeper into the accuracy of time-series tree cover map datasets was  
122 hindered.

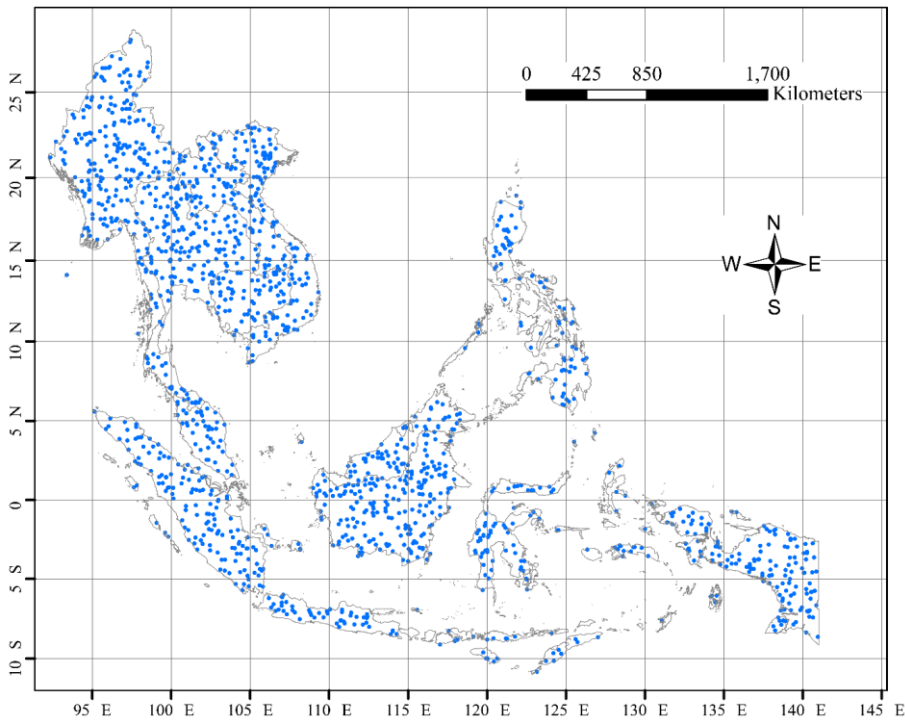
123

124 Following the methodology established by Yang et al. (2023), we undertook a rigorous process to generate a  
125 robust validation dataset for our study. Firstly, we randomly generated 1,515 points to ensure a representative  
126 sample of collected visual data, as illustrated in Fig. 1. Next, to classify these points as trees or non-trees, we  
127 enlisted four human interpreters and employed Planet Explorer within QGIS. Our approach involved visually  
128 identifying tree cover/non-tree cover pixels in the true color composite of Planet-NICFI imagery where the  
129 points were located. To ensure accuracy, we superimposed the 10 m tree height data, previously developed  
130 by Lang et al. (2022), onto the Planet-NICFI imagery. This step ensured that the labels adhered to the specified  
131 tree height criteria (i.e.,  $\geq 5$  m). Subsequently, we thoroughly evaluated and refined the labels using Google  
132 Earth. To make time series tree cover/non-tree cover labels, we maintained the geographic location of the  
133 1,515 points and changed the year of the Planet-NICFI imagery. The resulting labels encompassed data from

Deleted: comprehensively

135 the years 2016, 2017, 2018, 2020, and 2021. [Detailed](#) information about the validation dataset can be  
136 presented in Table 1.

Deleted: Comprehensive



137  
138 **Figure 1.** Spatial distribution of randomly generated 1,515 validation dataset points.

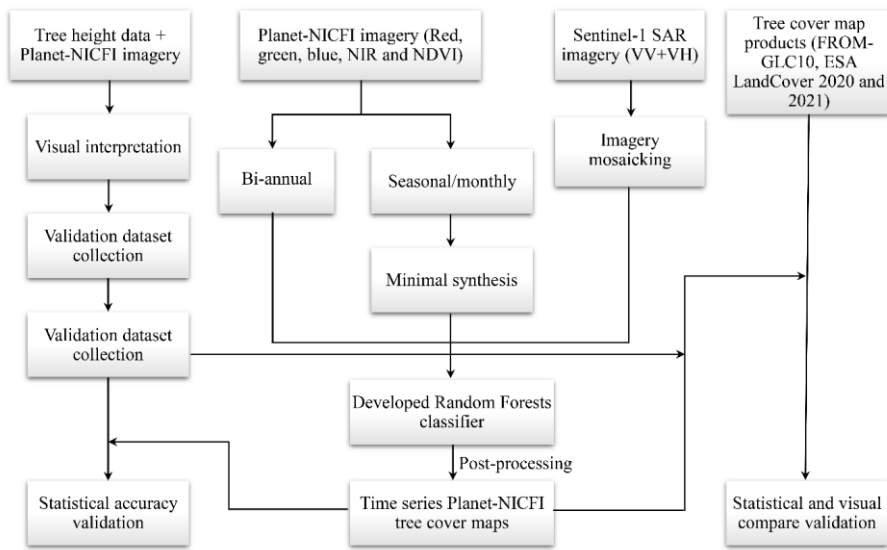
139  
140 **Table 1** Information of the mapped validation dataset for evaluating the generated tree cover map product.

Period	Count of sample points		
	Tree cover	Non-tree cover	Total
2016	1,086	429	1,515
2017	1,026	489	1,515
2018	977	538	1,515
2020	1,093	422	1,515
2021	952	563	1,515

141

143 **2.3 Methods**

144 We integrated Planet-NICFI and Sentinel-1 SAR imagery to generate a high-resolution (4.77 m) annual tree  
145 cover map product for SEA covering the years 2015-2021. Our framework involved several key steps,  
146 including defining mapped objects, preprocessing of imagery, and generation of time-series tree cover map  
147 product. The detailed workflow is illustrated in Fig. 2.



148 **Figure 2.** Workflow of generating tree cover map product for 2016-2021, including imagery preprocessing,  
149 generation of tree cover map product, and accuracy validation.

151  
152 **2.3.1 Definition of mapped tree cover**

153 Traditionally, forests are considered to meet specific criteria (tree cover and height). The Food and Agriculture  
154 Organization (FAO) of the United Nations defines forests as land spanning more than 0.5 hectares with trees  
155 higher than 5 m and a canopy cover above 10% (FAO, 2020). According to the United Nations Framework  
156 Convention on Climate Change (UNFCCC), forests are defined as areas with a minimum canopy cover of  
157 10-30%, minimum tree height of 2-5 m, and a minimum area of 0.1 ha (Parker et al., 2008).



158

159 In this study, tree cover is defined as any geographic area dominated by trees without a percentage of tree  
160 coverage at the pixel level (Zanaga et al., 2020; Hansen et al., 2013). This is attributed to the fact that the  
161 resolution of the Planet pixel (4.77 m) is closer to the size of trees in tropical areas. Next, we utilized Planet-  
162 NICFI imagery to generate only a prototype tree cover map with a resolution of 4.77 m and trees higher than  
163 5 m. Our tree cover map product serves as baseline data for forest cover analysis. Upon further development  
164 of the map to include trees higher than 5/2-5 m, it can be utilized for deriving forest cover maps for various  
165 functions, such as those provided by FAO and UNFCCC.

166

### 167 2.3.2 Preprocessing of imagery

168 We utilized the GEE platform to preprocess Planet-NICFI imagery and Sentinel-1 SAR data for generating  
169 tree cover maps for the years 2016-2021 (Fig. 2). Specifically, following the methodology of Yang et al.  
170 (2023), we first employed the `ee.ImageCollection.mosaic()` function to merge and assemble overlapping  
171 Sentinel-1 SAR data over the specified time period into a seamless, continuous imagery. Subsequently, we  
172 performed bilinear resampling on the SAR imagery, specifically the VV and VH bands, to match the spatial  
173 resolution of Planet-NICFI imagery with a spatial resolution of 4.77 m.

174

175 Planet-NICFI offers imagery at two different temporal frequencies spanning from 2016 to 2021. This includes  
176 semi-annual imagery from 2016 to 2019 and monthly data from 2020 to 2021. To create a coherent and  
177 consistent dataset for 2020 and 2021, we synthesized the selected time window of monthly imagery into  
178 single imagery for each band, namely red, green, blue, and near-infrared bands. Specifically, we utilized the  
179 `ee.ImageCollection.min()` function on each monthly imagery to extract the minimum monthly imagery, which

180 was then used to generate the second semi-annual imagery for 2020 and 2021. This approach was employed  
181 to minimize the impact of cloud pollution on Planet-NICFI imagery (Oishi et al, 2018).

182

### 183 2.3.3 Generation of time-series tree cover map product

184 In addition to applying the RF approach in our tree cover mapping (Yang et al., 2023), RF-based methods  
185 have been widely employed to develop global LCLUC products and show good performance (Zanaga et al.,  
186 2022; Zanaga et al., 2021; Buchhorn et al., 2020). To acquire the time-series tree cover map dataset, our  
187 methodology involved a two-step process. Initially, we integrated our custom RF approach, implemented on  
188 Google Earth Engine (GEE), with a cloud-based machine learning platform. This combination enabled us to  
189 obtain semi-annual Planet-NICFI and Sentinel-1 imageries spanning the years 2016 to 2021, as illustrated in  
190 Fig. 2. Following data acquisition, we performed several post-processing steps to generate accurate tree cover  
191 map product for the SEA region. These steps included downloading the acquired data from the cloud platform  
192 to a local location, conducting mosaic operations, clipping relevant areas, applying projection transformations,  
193 and performing correlation statistics. By employing this approach, we produced a high-resolution tree cover  
194 map product.

Deleted: comprehensive

Deleted: successfully

195

### 196 2.3.4 Statistical accuracy assessment

197 We used two methods to assess the statistical accuracy of our tree cover map product. The generated tree  
198 cover map product was compared pixel by pixel with the tree cover/non-tree cover labels. We then obtained  
199 a confusion matrix, including true tree cover (TP), true non-tree cover (TN), false tree cover (FP), and false  
200 non-tree cover (FN). These four values were used to calculate the user's accuracy, producer's accuracy, and  
201 overall accuracy at a 95% confidence level (Olofsson et al., 2014) and the F1 score based on Eqs. (1)-(4),  
202 respectively. Note that we opted against utilizing the Kappa coefficient for accuracy assessment due to its

205 [unsuitability for mapping error evaluation \(Pontius Jr et al., 2011; Allouche et al., 2006\).](#)

$$\text{User's accuracy (UA)} = \frac{TP}{TP + FP} \quad (1)$$

$$\text{Producer's accuracy (PA)} = \frac{TP}{TP + FN} \quad (2)$$

$$\text{Overall accuracy} = \frac{TP + TN}{TP + TN + FP + FN} \quad (3)$$

$$\text{F1 score} = \frac{2 \times UA \times PA}{UA + PA} \quad (4)$$

206

207 In addition, following Tsendbazar et al. (2021), we used a stability index based on the user's and producer's  
208 accuracy to evaluate the time-series accuracy consistency of the tree cover map product. The stability index  
209 used to evaluate tree cover accuracy is expressed as

$$SI_{t1} = \frac{|TC_{t1} - TC_{t1-1}|}{TC_{t1-1}} \times 100 \quad (5)$$

210 where  $SI_{t1}$  is the stability index that indicates the accuracy of tree cover maps (user's or producer's accuracy)  
211 at time  $t1$ ,  $TC_{t1}$  is tree cover accuracy at time  $t1$  and  $TC_{t1-1}$  is tree cover accuracy at the previous time ( $t0$   
212 or the reference year). We also used the maximum and average stability index for two consecutive years to  
213 assess the stability of our tree cover map product over a long period.

214

### 215 **3 Results**

216 We employed two approaches to assess the performance of our Planet-NICFI 2016-2021 tree cover map  
217 product. Firstly, we estimated the accuracy of our tree cover map product for each year to gain insights into  
218 their accuracy and consistency, based on the method developed by Tsendbazar et al. (2021). Additionally, we  
219 presented illustrative time series tree cover maps and documented the dynamics in tree cover area changes  
220 during the 2016-2021 period. Secondly, we compared our tree cover map product to widely used global tree  
221 cover map products at 10 m resolution, including FROM-GLC10 in 2017 (Gong et al., 2019), as well as ESA

222 WorldCover 2020 and 2021 (Zanaga et al., 2022; Zanaga et al., 2021).

223

### 224 3.1 Assessment of tree cover map product

225 We reported the annual accuracy of the time-series Planet-NICFI tree cover map product in Table 2 with a  
226 95% confidence level. The tree cover accuracy results for 2019 were provided by Yang et al. (2023). The  
227 overall accuracy of the tree cover map product ranged between  $0.867-0.907 \pm 0.015$  from 2016 to 2021, with  
228 the highest accuracy of  $0.907 \pm 0.014$  in 2021 and the lowest accuracy of  $0.867 \pm 0.017$  in 2016 (Table 2). This  
229 discrepancy may be due to poor data in the Planet-NICFI imagery during 2016 (Roy et al., 2021). The F1  
230 score showed a similar trend from 2016 to 2021, with an average of approximately 0.921. The user's accuracy  
231 consistently exceeded  $0.901 \pm 0.017$  over the six years, except for 2016 when it was  $0.862 \pm 0.021$ . The  
232 producer's accuracies were all higher than  $0.912 \pm 0.014$  (Table 2). Nevertheless, the mapping results of our  
233 time-series Planet-NICFI tree cover maps were highly consistent. Additionally, compared to the tree cover,  
234 the non-tree cover showed lower user's accuracy, producer's accuracy, and F1 score (i.e., approximately  
235  $0.856 \pm 0.027$ ,  $0.852 \pm 0.025$ , and 0.853, respectively), likely due to the complex composition of non-tree cover  
236 types, such as shrubland and herbaceous wetland.

237

238 **Table 2** User's accuracies, producer's accuracies, F1 score, and overall accuracies of the Planet-NICFI V1.0  
239 2016-2021 tree cover map product for SEA at a 95% confidence level. The accuracy evaluation results in  
240 2019 were provided by Yang et al. (2023).

Year	Classification	User's accuracy	Producer's accuracy	F1 score	Overall accuracy
2016	Tree cover	$0.862 \pm 0.021$	$0.925 \pm 0.018$	0.892	$0.867 \pm 0.017$
	Non-tree cover	$0.876 \pm 0.031$	$0.783 \pm 0.026$	0.827	
2017	Tree cover	$0.901 \pm 0.017$	$0.935 \pm 0.016$	0.917	$0.892 \pm 0.016$
	Non-tree cover	$0.874 \pm 0.033$	$0.814 \pm 0.027$	0.843	
2018	Tree cover	$0.929 \pm 0.016$	$0.912 \pm 0.014$	0.920	$0.892 \pm 0.015$
	Non-tree cover	$0.816 \pm 0.033$	$0.85 \pm 0.030$	0.832	
2019	Tree cover	$0.913 \pm 0.012$	$0.933 \pm 0.010$	0.923	$0.895 \pm 0.011$
	Non-tree cover	$0.857 \pm 0.022$	$0.819 \pm 0.021$	0.837	

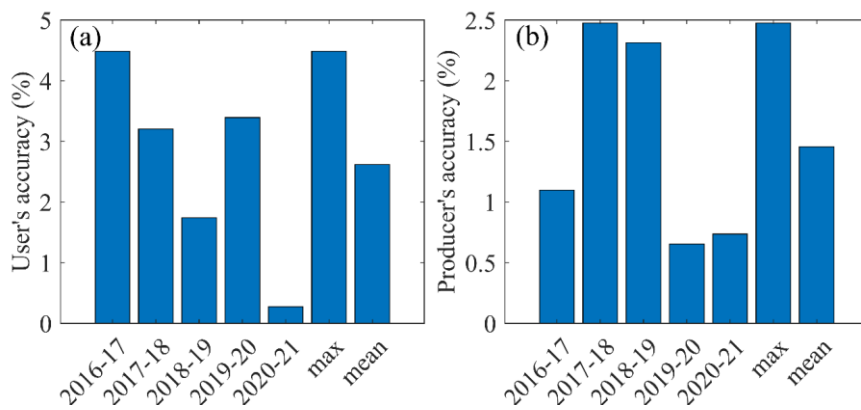
2020	Tree cover	0.944±0.014	0.927±0.011	0.935	0.900±0.014
	Non-tree cover	0.754±0.041	0.803±0.040	0.778	
2021	Tree cover	0.947±0.014	0.934±0.011	0.940	0.907±0.014
	Non-tree cover	0.778±0.038	0.816±0.039	0.796	

241

242 We also estimated the stability of our Planet-NICFI tree cover maps accuracy over 2016-2021 (Fig. 3). The

243 results show that the user's and producer's stability indexes were low than 4.5% and 2.5%, respectively,

244 indicating the good stability of our mapped Planet-NICFI tree cover maps for the six years (2016-2021).



245 **Figure 3.** Stability index estimates for the Planet-NICFI tree cover map product 2016-2021: the stability

246 index for (a) the user's accuracy and (b) the producer's accuracy.

247

248

249 We further visually compared our time-series tree cover map product with the original Planet-NICFI imagery

250 during 2016-2019 (Figures 4-5). Note that we have not shown the years 2020 and 2021 due to inconvenient

251 visualization for monthly resolution Planet-NICFI imagery collected from QGIS. In comparison, our tree

252 cover map product showed better consistencies with Planet-NICFI imagery, such as roads, the spatial

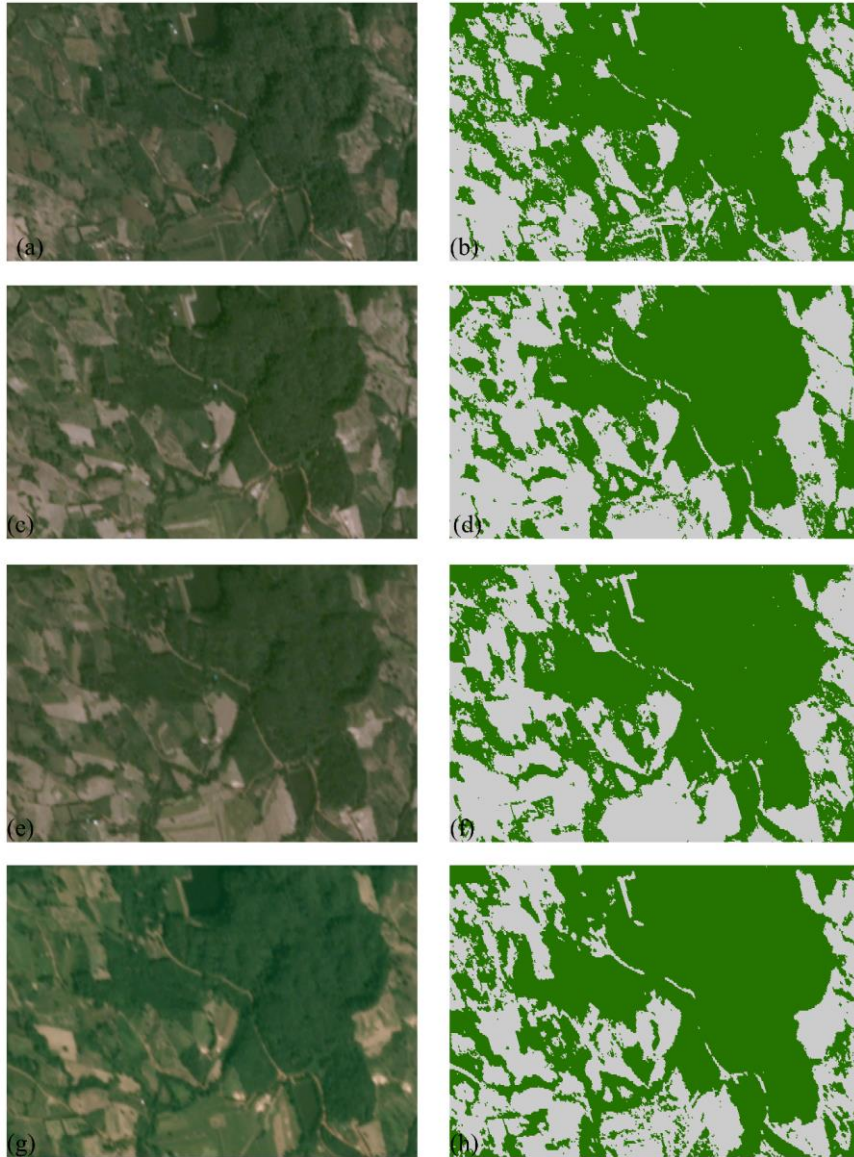
253 distribution pattern of tree cover, and non-tree cover. However, our tree cover product potentially exhibited

254 a "salt and pepper" phenomenon in some years (i.e., 2017 and 2018) due to the employment of the RF

255 approach. In practical applications, we need to pay attention to this phenomenon. In addition, we counted the

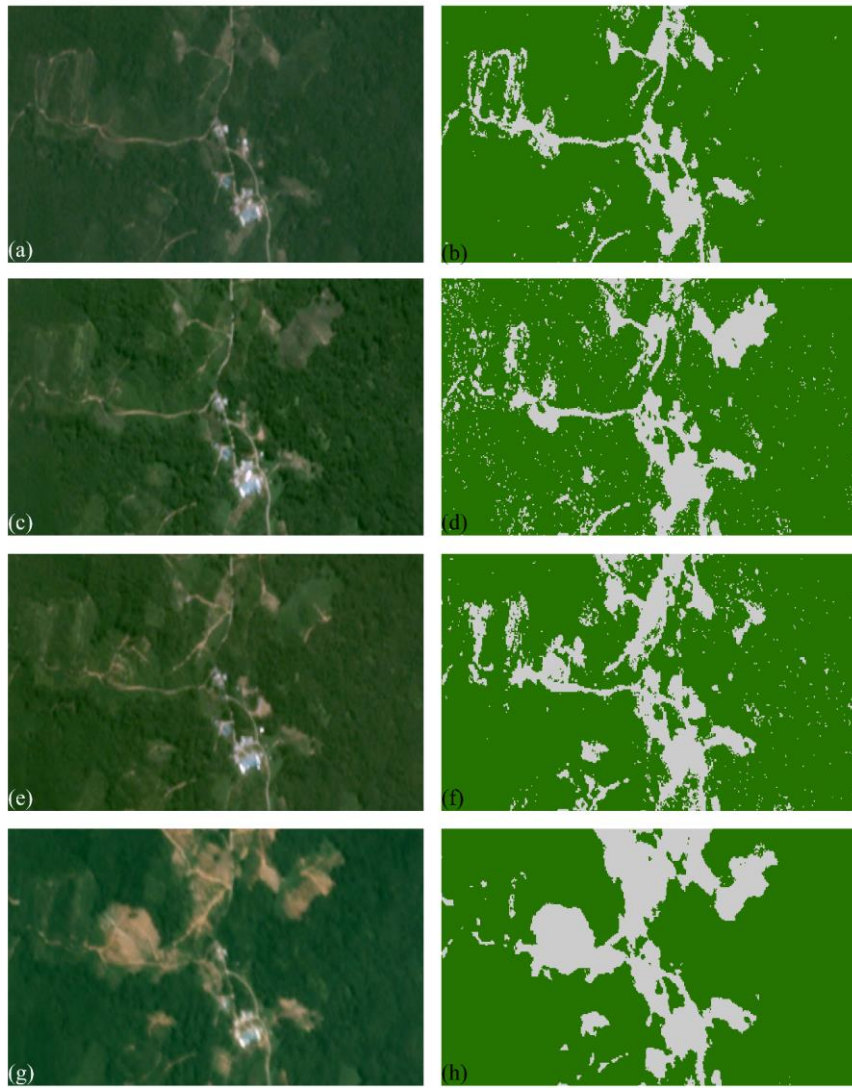
256 time series of the area estimates of tree cover maps during 2016-2021 and showed a slight increase trend

257 from 2016 to 2021, which is in line with the area estimates of ESA tree cover for the years 2020 and 2021.  
258 This may be due to forest restoration after the 2015 El Niño phenomenon (Wigneron et al., 2020), as well as  
259 the impact of expanded plantations (Xu et al., 2020).



260  
 261 **Figure 4.** Comparison of the time series of the derived tree cover maps (left column) and Planet-NICFI  
 262 imagery (right column) for the selected mainland SEA area (100.301°-100.322°E, 18.400°-18.409°N). (a)  
 263 and (b), (c) and (d), (e) and (f), and (g) and (h) indicate 2019, 2018, 2017, and 2017, respectively.

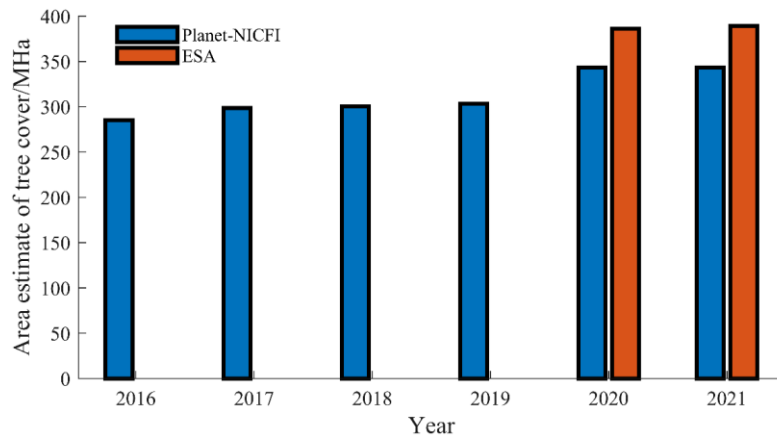
Deleted: Time



265  
 266 **Figure 5.** Comparison of the time series of the derived tree cover maps (left column) and Planet-NICFI  
 267 imagery (right column) for the selected maritime SEA area (111.789°-111.806°E, 2.032°-2.040°N). (a) and  
 268 (b), (c) and (d), (e) and (f), and (g) and (h) indicate 2019, 2018, 2017, and 2017, respectively.

Deleted: Time



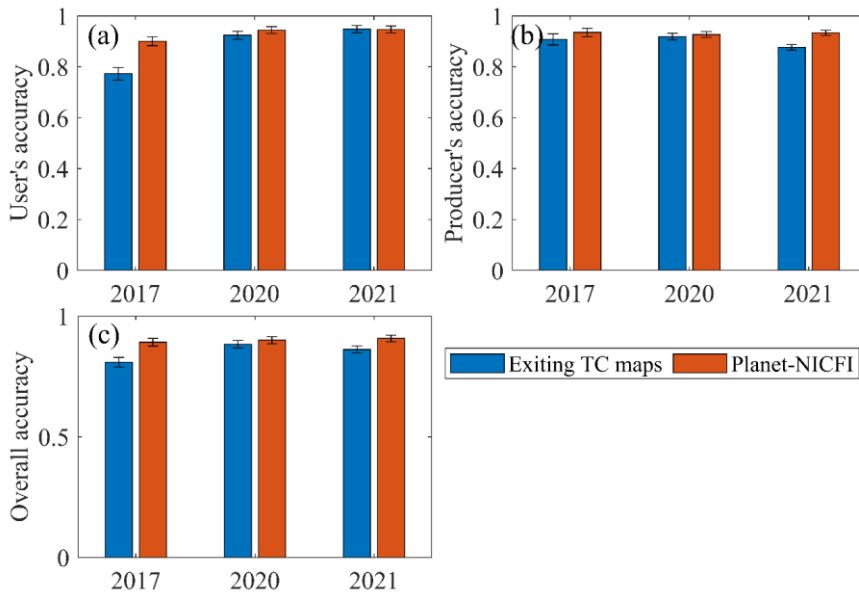


271 **Figure 6.** Area dynamics change of tree cover maps for Planet-NICFI and ESA from 2016 to 2021.  
 272

273

274 **3.2 Comparison with existing tree cover map products**

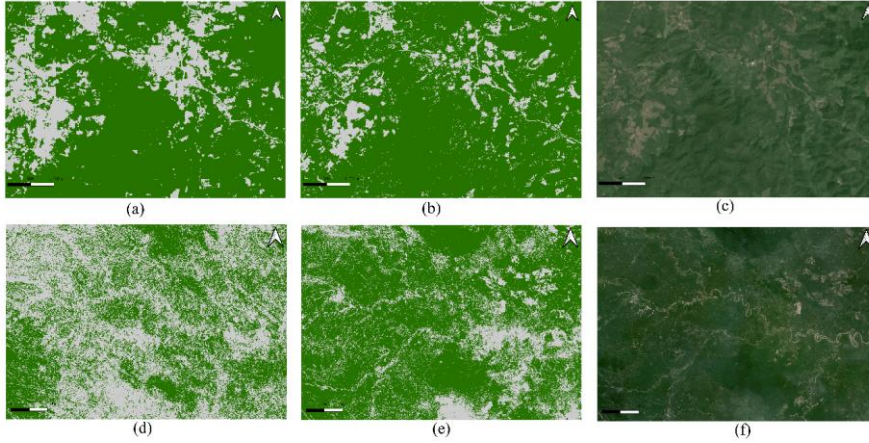
275 We compared our mapped Planet-NICFI tree cover maps with FROM-GLC10, ESA WorldCover 2020 and  
 276 2021 regarding statistical accuracy (Fig. 4). The results show that our tree cover maps outperformed FROM-  
 277 GLC10 in user’s accuracy, producer’s accuracy, and overall accuracy. The user’s accuracy and overall  
 278 accuracy of our tree cover maps exceeded 0.083. ESA WorldCover 2020 and 2021 showed similar  
 279 performances to our Planet-NICFI tree cover maps. Particularly, the user’s accuracy, producer’s accuracy,  
 280 and overall accuracy of ESA WorldCover 2020 decreased by 0.020, 0.008, and 0.017, respectively (Fig. 4).  
 281 This may be because we all used the SAR imagery as input and applied the RF-based machine learning  
 282 method to classify our tree cover.



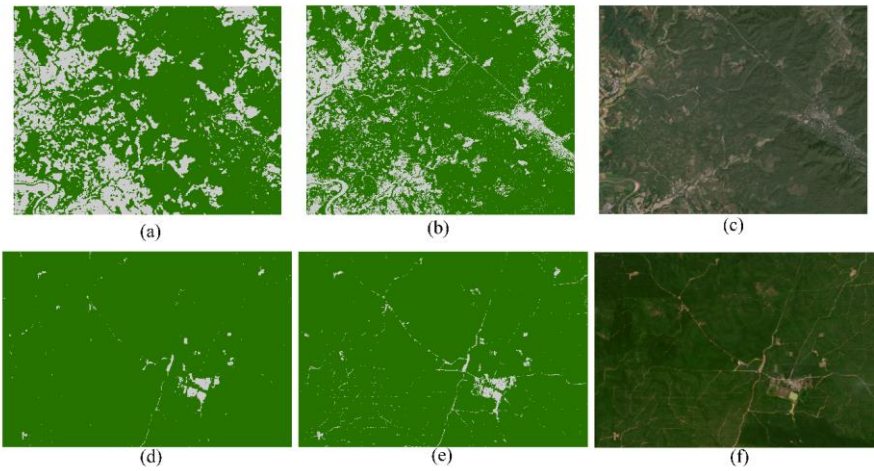
283 **Figure 7.** Accuracy comparison between existing tree cover maps and the generated Planet-NICFI tree cover  
 284 maps at a 95% confidence level: (a) user's accuracy, (b) producer's accuracy, and (c) overall accuracy.

286

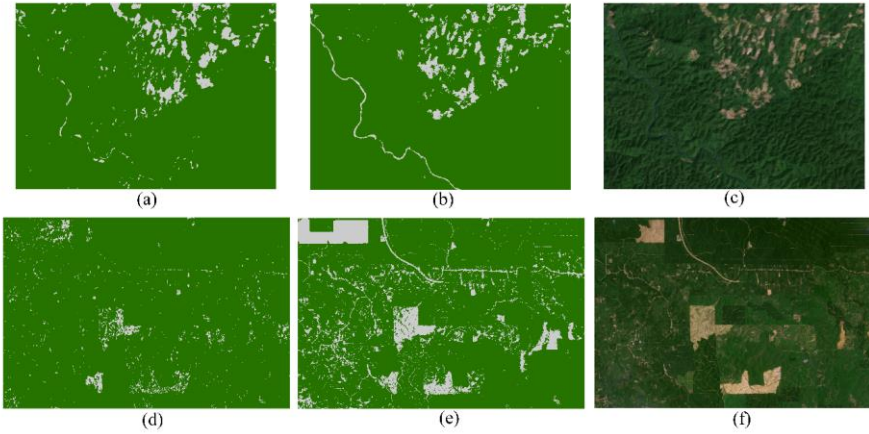
287 We selected six locations (three mainland SEA areas and three maritime SEA areas) to visually compare our  
 288 Planet-NICFI tree cover maps with three other 10-meter products, namely, FROM-GLC10, ESA WorldCover  
 289 2020 and 2021 (Figs. 8-10). In comparison, it is easier for FROM-GLC10 to classify all mixed tree and non-  
 290 tree areas into non-tree cover maps (Fig. 8a). This may be because FROM-GLC10 cannot apply SAR imagery  
 291 to tree cover mapping. However, ESA WorldCover 2020 and 2021 can capture tree cover landscapes at a  
 292 higher level of detail than FROM-GLC, such as long narrow roads, croplands, and built-up areas (Figs. 9-  
 293 10a). It should be noted that ESA WorldCover 2020 and 2021 omitted some long narrow non-tree cover  
 294 landscapes and small isolated tree cover and non-tree cover landscapes due to the limitation of the imagery  
 295 resolution (10 m).



296  
 297 **Figure 8.** Comparison of FROM-GLC10 (a) and (d), Planet-NICFI tree cover (b) and (e), and Planet-NICFI  
 298 imagery (c) and (f) for mainland SEA area (101.594°-101.651°E, 19.254°-19.294°N; top row) and maritime  
 299 SEA area (101.925°-103.296°E, -2.096°-1.145°S; bottom row). Green and gray 20% indicate tree cover and  
 300 non-tree cover, respectively.  
 301



302  
 303 **Figure 9.** Comparison of ESA WorldCover 2020 (a) and (d), Planet-NICFI tree cover (b) and (e), and Planet-  
 304 NICFI imagery (c) and (f) for mainland SEA area (98.310°-98.392°E, 17.102°-17.166°N; top row) and  
 305 maritime SEA area (99.983°-100.064°E, 1.387°-1.442°N; bottom row). Green and gray 20% indicate tree  
 306 cover and non-tree cover, respectively.  
 307



308  
 309 **Figure 10.** Comparison of ESA WorldCover 2021 (a) and (d), Planet-NICFI tree cover (b) and (e), and Planet-  
 310 NICFI imagery (c) and (f) for Mainland SEA area (102.179°-102.249°E, 18.676°-18.726°N; top row) and  
 311 maritime SEA area (99.951°-100.063°E, 1.892°-1.967°E; bottom row). Green and gray 20% indicate tree  
 312 cover and non-tree cover, respectively.  
 313

#### 314 4 Discussion

315 Our time-series Planet-NICFI tree cover map product was mapped twice a year to mitigate the impact of  
 316 smog, light, cloud, and topographic effects in tropical areas (Roy et al., 2021; Marta et al., 2018). This high-  
 317 resolution tree cover map product meets the minimum tree height requirement of  $\geq 5$  m for further generating  
 318 forest data. However, it should be noted that we cannot guarantee 100% tree cover for each higher-resolution  
 319 pixel, which may introduce some uncertainties when using the higher-resolution tree cover maps. Despite  
 320 excluding plantations during sample point labeling, some plantations, such as oil palm, may still be mixed  
 321 into our tree cover map product due to similarities in anomalies (Mugabowindekwe et al., 2023; Zanaga et  
 322 al., 2022; Zanaga et al., 2021). As a result, caution should be exercised when using our Planet-NICFI tree  
 323 cover map product for certain purposes.

324  
 325 To generate a high-resolution time series tree cover map product at a continental scale, we utilized advanced

326 random forests-based machine learning algorithms on the GEE platform. However, for fine-scale tree cover  
327 mapping, deep learning-based segmentation methods, such as U-net (Falk et al., 2019), are necessary,  
328 particularly when using limited bands (Mugabowindekwe et al., 2023; Wagner et al., 2023; Zanaga et al.,  
329 2022; Zanaga et al., 2021; Brandt et al., 2020). As a result, our tree cover map product still has some  
330 uncertainty due to limitations in the optical PlanetScope imagery. Additionally, our tree cover map product  
331 has the potential to display a salt and pepper phenomenon in certain locations and years, attributed to the  
332 utilization of the RF method. To improve our tree cover mapping product with higher accuracy, we need to  
333 consider adding more bands or utilizing advanced deep learning algorithms in the future.

Deleted: resolution

334

## 335 **5 Data availability**

336 The high-resolution Planet-NICFI V1.0 time-series tree cover product is now available at  
337 <https://cstr.cn/31253.11.sciencedb.07173> (Yang and Zeng, 2023). This product is provided in the Mollweide  
338 projection and the World Geodetic System 1984 (WGS1984) datum and geographic coordinate system. Tree  
339 cover and non-tree cover are denoted as 0 and 1, respectively, in each yearly file, and are stored as UINT8 in  
340 GeoTIFF format. The GeoTIFF files are named Planet-FC\_SEA\_<YEAR>\_prj.tif, for example, Planet-  
341 FC\_SEA\_16\_prj.tif.

342

## 343 **6 Conclusions**

344 We have successfully generated the first accurate and high-resolution time-series tree cover map product for  
345 SEA by combining optical and SAR satellite observations, utilizing advanced random forests machine  
346 learning algorithms on the GEE platform. Our Planet-NICFI tree cover map product exhibits excellent  
347 accuracy and consistency over six years (2016-2021). The baseline tree cover map product, with a resolution

349 of 4.77 m, can be easily converted to forest cover maps at different resolutions to cater to the diverse needs  
350 of users. Moreover, our tree cover map product has the unique ability to address rounding errors in forest  
351 cover mapping by accurately capturing isolated trees and monitoring the removal of long, narrow forest cover.  
352 These cutting-edge fine-scale time-series tree cover maps represent a milestone in forest monitoring and offer  
353 unprecedented opportunities for users across diverse disciplines.

354

### 355 **Code Availability**

356 The scripts used to generate all Planet-NICFI v1.0 tree cover 2016-2021 are provided in JavaScript  
357 ([https://code.earthengine.google.com/?scriptPath=users%2Fyfitaorus%2Fcodes%3APlanet\\_RF-LC\\_rac](https://code.earthengine.google.com/?scriptPath=users%2Fyfitaorus%2Fcodes%3APlanet_RF-LC_rac)).

358 The maps can be automatically generated by running the codes. The scripts are also available on request from  
359 Z. Zeng.

360

### 361 **Acknowledgments**

362 This study was supported by the National Natural Science Foundation of China (grant no. 42071022), the  
363 start-up fund provided by the Southern University of Science and Technology (no. 29/Y01296122), and the  
364 China Postdoctoral Science Foundation (grant no. 2022M711472). We thank Sen Jiang, Haowen Duan, Hao  
365 Li, and Fangdong Fu for making tree cover/non-tree cover label data that are used to assess the time series  
366 tree cover map products.

367

### 368 **Author contributions**

369 Z.Z. designed the research; F.Y. performed the analysis and wrote the draft. All authors contributed to the

370 interpretation of the results and the writing of the paper.

371

372 **Competing interests**

373 The authors declare no competing interests.

374 **References**

- 375 Achard, F., Beuchle, R., Mayaux, P. et al.: Determination of tropical deforestation rates and related carbon  
376 losses from 1990 to 2010, *Glob Chang Biol*, 20(8), 2540-2554, 2014.
- 377 [Allouche, O., Tsoar, A., Kadmon, R.: Assessing the accuracy of species distribution models: prevalence,  
378 kappa and the true skill statistic \(TSS\), \*J. Appl. Ecol.\*, 43\(6\), 1223-1232, 2006.](#)
- 379 Brandt, M., Tucker, C. J., Kariryaa, A., et al.: An unexpectedly large count of trees in the West African Sahara  
380 and Sahel, *Nature*, 587(7832), 78-82, 2020.
- 381 Buchhorn, M., Lesiv, M., Tsendbazar, N. E., et al.: Copernicus global land cover layers—collection 2, *Remote  
382 Sens.*, 12(6), 1044, 2020.
- 383 Chen, J., Chen, J., Liao, A., et al.: Global land cover mapping at 30 m resolution: A POK-based operational  
384 approach. *ISPRS J. Photogramm, Remote Sens.*, 103, 7-27, 2015.
- 385 CoP26, G. L.: Glasgow Leaders' Declaration on Forests and Land Use. Available online at: [https://ukcop26.  
386 org/glasgow-leaders-declaration-on-forests-and-land-use/](https://ukcop26.org/glasgow-leaders-declaration-on-forests-and-land-use/)(accessed December 06, 2021).
- 387 ESA: Land Cover CCI Product User Guide Version 2. Tech. Rep. Available at:  
388 [maps.elie.ucl.ac.be/CCI/viewer/download/ESACCI-LC-Ph2-PUGv2\\_2.0.pdf](https://maps.elie.ucl.ac.be/CCI/viewer/download/ESACCI-LC-Ph2-PUGv2_2.0.pdf), 2017.
- 389 Falk, T., Mai, D., Bensch, R., et al. U-Net: deep learning for cell counting, detection, and morphometry, *Nat.  
390 Methods*, 16(1), pp.67-70, 2019.
- 391 FAO: Global forest resources assessment 2020: Main report. Technical report, Food and Agriculture  
392 Organization of the United Nations, ROME, 2020.
- 393 Feng, Y., Ziegler, A. D., Elsen, P. R., et al.: Upward expansion and acceleration of forest clearance in the  
394 mountains of Southeast Asia, *Nat. Sustain*, 4(10), 892-899, 2021.
- 395 Friedl, M., Sulla-Menashe, D.: MCD12Q1 MODIS/Terra+Aqua Land Cover Type Yearly L3 Global 500m  
396 SIN Grid V006. NASA EOSDIS Land Processes DAAC. Accessed 2022-12-15 from  
397 <https://doi.org/10.5067/MODIS/MCD12Q1.006>, 2019.
- 398 Gong P., Liu H., Zhang M., et al.: Stable classification with limited sample: Transferring a 30-m resolution  
399 sample set collected in 2015 to mapping 10-m resolution global land cover in 2017, *Sci. Bull*, 64, 370-  
400 373, 2019.
- 401 Gorelick, N., Hancher, M., Dixon, M., et al.: Google Earth Engine: Planetary-scale geospatial analysis for  
402 everyone, *Remote Sens. Environ.*, 202, 18-27, 2017.
- 403 Hammer, D., Kraft, R., Wheeler, D.: Alerts of forest disturbance from MODIS imagery, *Int J Appl Earth Obs  
404 Geoinf*, 33, 1-9, 2014.
- 405 Hansen, M. C., Potapov, P. V., Moore, R., et al.: High-resolution global maps of 21st-century forest cover  
406 change, *Science*, 342(6160), 850-853, 2013.
- 407 Hansen, M. C., Stehman, S. V., Potapov, P. V.: Quantification of global gross forest cover loss, *Proc Natl  
408 Acad Sci USA*, 107(19), 8650-8655, 2010.
- 409 Hsieh, P. F., Lee, L. C., Chen, N. Y.: Effect of spatial resolution on classification errors of pure and mixed  
410 pixels in remote sensing, *IEEE Trans. Geosci. Remote Sens.*, 39(12), 2657-2663, 2001.
- 411 Karra K., Kontgis C., Statman-Weil Z., et al.: Global land use/land cover with Sentinel 2 and deep learning.  
412 In 2021 IEEE international geoscience and remote sensing symposium IGARSS (pp. 4704-4707), IEEE,  
413 2021, July.
- 414 Lang, N., Jetz, W., Schindler, K. Wegner, J. D.: A high-resolution canopy height model of the Earth,  
415 doi:10.48550/arxiv.2204.08322, 2022.
- 416 Marta, S.: Planet imagery product specifications, Planet Labs: San Francisco, CA, USA, 91, 2018.



417 Mugabowindekwe, M., Brandt, M., Chave, J., et al.: Nation-wide mapping of tree-level aboveground carbon  
418 stocks in Rwanda, *Nat. Clim. Change*, 1-7, 2023.

419 Oishi, Y., Sawada, Y., Kamei, A., et al.: Impact of Changes in Minimum Reflectance on Cloud Discrimination,  
420 *Remote Sens.*, 10(5), 693, 2018.

421 Olofsson, P., Foody, G.M., Herold, M., et al.: Good practices for estimating area and assessing accuracy of  
422 land change, *Remote Sens. Environ.*, 148, 42-57, 2014.

423 Parker, C., Mitchell, A., Trivedi, M., Mardas, N.: The little REDD book: a guide to governmental and non-  
424 governmental proposals for reducing emissions from deforestation and degradation. The little REDD  
425 book: a guide to governmental and non-governmental proposals for reducing emissions from  
426 deforestation and degradation,  
427 [http://www.globalcanopy.org/themedia/file/PDFs/LRB\\_lowres/lrb\\_en.pdf](http://www.globalcanopy.org/themedia/file/PDFs/LRB_lowres/lrb_en.pdf), 2008.

428 Planet Team: Planet Application Program Interface: In Space for Life on Earth. San Francisco, CA,  
429 <https://api.planet.com>, 2017.

430 [Pontius Jr, R. G., Millones, M.: Death to Kappa: birth of quantity disagreement and allocation disagreement  
431 for accuracy assessment, \*Int. J. Remote Sens.\*, 32\(15\), 4407-4429, 2011.](#)

432 Reiner, F., Brandt, M., Tong, X., et al.: More than one quarter of Africa's tree cover found outside areas  
433 previously classified as forest, [Nat Commun, 14, 2258 \(2023\).](#)

434 Roy, D.P., Huang, H., Houborg, R., Martins, V.S.: A global analysis of the temporal availability of  
435 PlanetScope high spatial resolution multi-spectral imagery, *Remote Sens. Environ.*, 264, 112586, 2021.

436 Sexton, J.O., Noojipady, P., Song, X.P., Feng, M., Song, D.X., Kim, D.H., Anand, A., Huang, C., Channan,  
437 S., Pimm, S.L., Townshend, J.R.: Conservation policy and the measurement of forests, *Nat. Clim.  
438 Change*, 6(2), 192-196, 2016.

439 Shimada, M., Itoh, T., Motooka, T., Watanabe, M., Shiraishi, T., Thapa, R., & Lucas, R.: New global  
440 forest/non-forest maps from ALOS PALSAR data (2007–2010), *Remote Sens. Environ.*, 155, 13-31,  
441 2014.

442 Skea J., Shukla P. R., Reisinger A., et al.: Climate change 2022: Mitigation of climate change, IPCC Sixth  
443 Assessment Report, 2022.

444 Tsendbazar, N., Herold, M., Li, L., et al.: Towards operational validation of annual global land cover maps,  
445 *Remote Sens. Environ.*, 266, 112686, 2021.

446 Velasco, R.F., Lippe, M., Tamayo, F., et al.: Towards accurate mapping of forest in tropical landscapes: A  
447 comparison of datasets on how forest transition matters, *Remote Sens. Environ.*, 274, 112997, 2022.

448 Wagner, F. H., Dalagnol, R., Silva-Junior, C. H., et al.: Mapping Tropical Forest Cover and Deforestation  
449 with Planet NICFI Satellite Images and Deep Learning in Mato Grosso State (Brazil) from 2015 to 2021,  
450 *Remote Sens.*, 15(2), 521, 2023.

451 Wigneron, J.P., Fan, L., Ciais, P., et al. Tropical forests did not recover from the strong 2015–2016 El Niño  
452 event, *Sci. Adv.*, 6(6), p.eaay4603, 2020.

453 Xu, Y., Yu, L., Li, W., et al. Annual oil palm plantation maps in Malaysia and Indonesia from 2001 to 2016,  
454 *Earth Syst. Sci. Data*, 12(2), pp.847-867, 2020.

455 Yang, F., Jiang X., Alan D. Ziegler, et al. Improved fine-scale tropical forest cover mapping for Southeast  
456 Asia using Planet-NICFI and Sentinel-1 imagery, *J. Remote Sens.*, 0,  
457 <https://doi.org/10.34133/remotesensing.0064>, 2023.

458 Zanaga D., Van De Kerchove R., Daems D., et al.: ESA WorldCover 10 m 2021 v200,  
459 <https://doi.org/10.5281/zenodo.7254221>, 2022.

460 Zanaga D., Van De Kerchove R., De Keersmaecker W., et al.: ESA WorldCover 10 m 2020 v100,

- 461 <https://doi.org/10.5281/zenodo.5571936>, 2021.
- 462 Zeng, Z., Estes, L., Ziegler, A. D., et al.: Highland cropland expansion and forest loss in Southeast Asia in  
463 the twenty-first century, *Nat. Geosci*, 11(8), 556-562, 2018a.
- 464 Zeng, Z., Gower, D. and Wood, E. F.: Accelerating Forest loss in Southeast Asian Massif in the 21st century:  
465 A case study in Nan Province, Thailand, *Glob Chang Biol*, 24, 4682-4695, 2018b.